Pergamon

Geochimica et Cosmochimica Acta, Vol. 68, No. 20, pp. 4113-4119, 2004

0016-7037/04 $30.00 + .00

doi:10.1016/j.gca.2003.11.031

Imaging and mechanical property measurements of kerogen via nanoindentation

JONATHAN C. ZESZOTARSKI,[1] RICHARD R. CHROMIK,[2] RICHARD P. VINCI,[2] MARIE C. MESSMER,[1] RAYMOND MICHELS,[3] and JOHN W. LARSEN[1,*,†]

[1]Department of Chemistry, Lehigh University, 6 East Packer Avenue, Lehigh University, Bethlehem, PA 18015, USA
[2]Department of Materials Science and Engineering, Lehigh University, 5 East Packer Avenue, Lehigh University, Bethlehem, PA 18015, USA
[3]CNRS-UMR 7566 G2R, Universite Henri Poincare, Faculte des Sciences, BP 23, 54501 Vandoeuvre les Nancy, France

(*Received April* 24, 2003; *accepted in revised form November* 21, 2003)

Abstract—Most analyses of kerogens rely on samples that have been isolated by dissolving the rock matrix. The properties of the kerogen before and after such isolation may be different and all sample orientation information is lost. We report a method of measuring kerogen mechanical properties in the rock matrix without isolation. An atomic force microscope (AFM) based nanoindenter is used to measure the hardness and reduced modulus of the kerogen within Woodford shale. The same instrument also provides useful images of polished rock sections on a submicrometer scale. Measurements were carried out both parallel and perpendicular to the bedding plane. *Copyright © 2004 Elsevier Ltd*

1. INTRODUCTION

In spite of significant research activity surrounding kerogen, fundamental questions remain regarding the forces shaping its macromolecular structure. Does kerogen exist in an isotropic environment controlled by the pressure within the fluid-filled pore structure of the source rock, or does kerogen experience an anisotropic environment dictated by the enormous pressure of the overbearing rock? This important question has bearing on the study of kerogen maturation and the modeling of hydrocarbon primary migration as discussed by Khorasani and Michelsen (1995) and references therein. Lewan et al. (1979) first studied artificial kerogen maturation by hydrous pyrolysis at water liquid-vapor equilibrium pressure. Burnham and Braun (1990) developed a detailed model of petroleum formation, destruction and expulsion based upon results of a number of techniques including hydrous pyrolysis. Blanc and Connan (1992) as well as Michels et al. (1994, 1995a, 1995b) showed that pressure was an important factor in the study of hydrocarbon generation and expulsion by confined pyrolysis, and Michels et al. (1995a, 1995b) showed pressure was important in hydrous pyrolysis as well. However, models of kerogen maturation and hydrocarbon primary migration have not achieved consensus on the use of pressure. Rudkiewicz et al. (1994) employed constant hydrostatic pressures in experiments on immature type II kerogen used to model migration behavior of hydrocarbons. On the other hand, Hanebeck (1995) showed that lithostatic pressure has an effect on kerogen maturation and oil primary migration. Accurately determining the pressure environment experienced by kerogen is important because the study of kerogen maturation and hydrocarbon primary migration is necessary for the generation of models to guide petroleum exploration and recovery.

An approach to studying the possible anisotropy of kerogen can be found in the analysis of oriented polymers. It is well known that even amorphous polymers will exhibit strain-induced orientation. For example, this orientation has been determined for polystyrene by birefringence measurements (Andrews, 1954) and hardness measurements (Fett et al., 1973). A geopolymeric example is coal, which has been analyzed for anisotropy by a number of techniques including solvent swelling (Cody et al., 1988), static and dynamic physical tests (Morgans and Terry, 1958), optical birefringence (van Krevelen, 1960) and nanoscale mechanical measurements (Yamada et al., 2000).

Evidence to answer the question of what forces are experienced by kerogen may be found in its properties as determined relative to the bedding plane. In relatively shallow sedimentary basins, lithostatic pressure is exerted along a vector directed toward the center of the earth and is therefore anisotropic (as opposed to deeper sections of the earth's crust, typically out of the range of sedimentary basins, where lithostatic pressure may be isotropic). Hydrostatic pressure is due to fluid that surrounds the kerogen evenly and is therefore isotropic. If the kerogen has been strained by lithostatic pressure, the resulting orientation of macromolecular chains should manifest itself as anisotropy in the mechanical properties of the kerogen.

However, to retain strain-induced orientation, the kerogen must stay glassy, that is, remaining at a temperature below its glass transition temperature (T_g). In a glassy polymer, the non-covalent interactions between molecular segments are so strong that they are not disrupted by the available thermal energy (Donath, 2001) and along with the covalent cross links, impede movement of the polymer chains. The strong intersegment forces result in a brittle polymer that is not capable of the rearrangement necessary to remove strain-orienting effects. Only two kerogens (Green River and Rundle) have had their physical state determined by solid-state NMR methods. Both are glassy at room temperature (Parks et al., 1988) and remain predominantly glassy through the oil window. Thus, it is expected that similar kerogens would retain structural anisotropy as the signature of exposure to significant lithostatic pressure.

Due to the fact that it exists as a minor component in the source rock, the analysis of kerogen has traditionally involved its isolation from the matrix. The procedures to isolate kerogen

* Author to whom correspondence should be addressed (jwl0@lehigh.edu).
† *Present address:* The Energy Institute, 209 Academic Projects Building, The Pennsylvania State University, University Park, PA 16802

(Göklen et al., 1984; Saxby, 1970) involve significant time investment with risks to sample purity and damage to the sample. Identifying the bedding plane in isolated kerogens would be difficult, if not impossible. Therefore, any analysis examining anisotropy requires that the kerogen be analyzed without removal of the matrix. The nature of its occurrence necessitates the use of analytical methods capable of probing a small sample size and the ability to distinguish the kerogen from its surrounding environment.

Nanoindentation is a method capable of achieving the dual goals of small sample size and contrast for the analysis of embedded kerogen. It is a refinement of indentation testing where the depth of penetration is on the order of nanometers rather than the microns or millimeters involved in conventional hardness testing. This shallow penetration is achieved through the use of a sensitive capacitance transducer system (Bhushan et al., 1996), allowing careful load control and sensitive determination of displacement. A distinguishing feature of nanoindentation testing is the indirect measurement of the contact area between the indenter tip and the specimen. Rather than direct measurement of an indentation's residual imprint, knowledge of the tip's geometry together with measurement of the depth of penetration allows the calculation of the contact area as a function of depth. For this reason, nanoindentation is sometime known as depth sensing indentation (Fischer-Cripps, 2002). This distinguishing feature of nanoindentation is especially important for the study of elastic materials, such as cross-linked polymers, since it avoids the errors associated with elastic recovery inherent in the traditional hardness testing methods. Nanoindentation can measure both the hardness and the elastic properties of a sample regardless of its elastic or plastic nature.

We use an atomic force microscope (AFM) modified to make mechanical property measurements by nanoindentation. Standard AFM has been used successfully to image Precambrian kerogen (Kempe et al., 2002). Instead of the traditional cantilever based AFM, we employ a diamond-tipped nanoindenter shaft. The nanoindenter tip is brought into contact with the surface of the shale and rastered across the surface to provide AFM imaging of somewhat lower quality than standard AFM. To perform nanoindentation, the force on the tip is increased and its movement distance into the sample is recorded as a function of the applied force. From the force vs. distance curve, hardness and elastic modulus of the solid can be derived. The image quality is sufficient to identify individual phases and to analyze the residual indentation. By examining samples cut parallel and perpendicular to the bedding plane, anisotropy of the hardness and elastic modulus of kerogen within the rock matrix was explored.

We chose to study kerogen within Woodford shale. Woodford shale is one of the major source rocks in the U. S. Midwest (Comer and Hinch, 1987; Burruss and Hatch, 1989; Johnson and Cardott, 1992; Kirkland et al., 1992). It extends from Kansas to Texas with its main occurrence in the state of Oklahoma (Anadarko Basin). Woodford shale is a clastic sedimentary formation deposited in an anaerobic marine environment during the Upper Devonian period. Its thickness reaches 300m in the deepest parts of the Anadarko basin (Oklahoma). It is rich in organic matter: the mean total organic content (TOC) ranges from 5.4 to 6.9 wt.% (Comer and Hinch, 1987), but can locally reach much higher values (up to 26 wt.%).

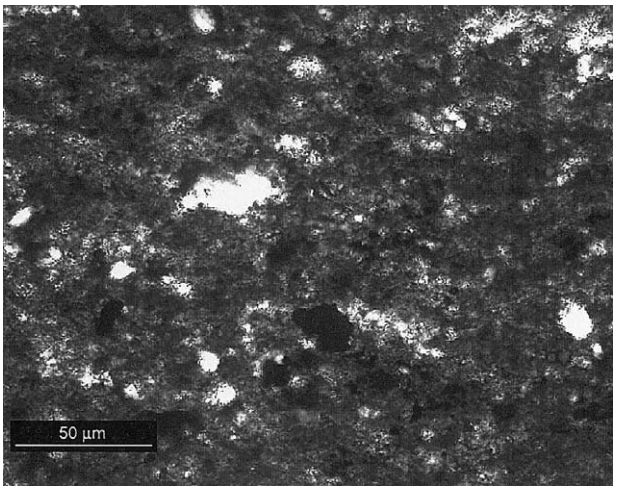

Fig. 1. A 500× magnification optical micrograph of a thin section sample of Woodford shale using transmitted light. Quartz and pyrite appear as large white and black regions, respectively. Kerogen is present in the grey matrix, with individual kerogen regions too small to be discernible at this magnification.

During the Pennsylvanian period, orogenic pulses induced strong subsidence of the Anadarko and neighbouring basins located in Oklahoma (Johnson and Cardott, 1992 and references therein). The Woodford shale thus displays maturity stages from immature to metamorphic (Comer and Hinch, 1987; Cardott and Lambert, 1985; Cardott, 1989). Maturity studies in the Anadarko basin suggest that source rock units have been in the oil and gas generation window almost continuously since late Paleozoic (Rice et al., 1989; Schmoker and Hester, 1989; Smith, 1989; Wang, 1989; Philp et al., 1992) and many oil occurrences are related to the maturation of the kerogen within Woodford shale (Jones, 1986; Philp et al., 1989; Reber, 1989; Jones and Philp, 1990).

2. EXPERIMENTAL MATERIALS AND METHODS

2.1. Materials

The Woodford shale used in this study was collected from an outcrop of the Woodford Formation located along I35, south of the Arbuckle Mountains (Carter County, Oklahoma; Kirkland et al., 1992). In the section sampled, the Woodford Formation presents strata of dark very fine-grained siltstone alternating with dark strongly silicified layers. The samples used in this study belong to the non-silicified strata and were collected from a freshly dug trench. Under the optical microscope, the samples appear as very finely laminated quartz-rich layers alternating with dark brown amorphous kerogen. Quartz and amorphous silica are the strongly dominant minerals. Pyrite grains are disseminated throughout the samples. Clay minerals are scarce and are mainly illite. An optical micrograph at maximum magnification is shown in Figure 1.

To ensure these samples are truly representative, geochemical characterization of the kerogen was performed. Kerogen, isolated by acid attack as required, was analysed by elemental analysis, Rock-Eval and FTIR spectroscopy. The characteristics of the organic matter in our Woodford shale sample are: TOC=22%, H/C=1.13, O/C=0.063 (%H=6.64; %O=6; %C=70.7; %N=2.56). Rock-Eval Hydrogen Index is 529 mg of hydrocarbons per gram of organic carbon, Oxygen Index is 5.32 mg of CO_2 per gram of organic carbon, T_{max} = 421°C. The chloroform soluble extract obtained by Soxhlet reflux for 48 h is 1 wt.% of the whole rock. Isolated kerogen was unable to be imaged due to its poor polishing characteristics. All geochemical data including

biomarker analysis indicate that the kerogen is of type II and is immature (Michels et al., 1994, 1995a, 1995b).

Cut and polished shale samples were used for nanoindentation measurements and imaging. Because the source of the samples is the flank of an anticline, the stress experienced by the samples is not uniformly vertical. However, according to estimations by Cardott et al. (1990), the location from which our Woodford shale sample was collected was buried to a maximum of 1.23 to 1.79 km (maximum of 0.47 kbar lithostatic pressure). By measuring the mechanical properties in three orthogonal directions (vide supra), anisotropy may still be detected. Two of the samples were cut perpendicular to the bedding plane and one was cut parallel. The samples, approximately 1 mm thick, were mounted on stainless steel discs and wet polished by hand with 0.3 μm alumina and 0.05 μm silica suspensions. After rinsing and sonicating briefly in deionized water (>16 MΩ resistivity), samples were allowed to air dry.

2.2. Methods

AFM images and nanoindentation experiments were performed using a Hysitron Triboscope two-dimensional transducer mounted on a Digital Instruments Multimode atomic force microscope equipped with a 100 μm X 100 μm scanner. The diamond indenter tip, a three-sided pyramid (Berkovich geometry) with a tip radius of approximately 150 nm, served as the AFM tip for imaging. The projected tip area as a function of contact depth in the range of interest and the load frame compliance were calibrated using a fused quartz standard following the procedure of Oliver and Pharr (1992).

Homogenous kerogen regions of 2 μm^2 or larger were selected for indentation. A minimum of 29 indentations were recorded for each sample. Indentation experiments consisted of loading at 0.25 mN/s to a maximum load of 1 mN. This maximum load was held for 3 s followed by unloading at 0.25 mN/s. The maximum depth of the indenter for this load was less than 400 nm. Concerns for edge effects from the elastic/plastic strain field beneath the indenter (Tsui et al., 1999; Chen and Vlassak, 2001) prevented use of larger loads or smaller regions of kerogen.

Determination of physical properties from nanoindentation experiments involves analysis of the generated load-displacement curves. The Oliver-Pharr method is used in this study to calculate hardness and reduced modulus values (Oliver and Pharr, 1992). The upper portion of the unloading data (in our case, data from 40 to 95% of the maximum load) is fit to a power law. The slope of the initial portion of this fit determines the stiffness, S (i.e., $S = dP/dh$, where P is the load and h the displacement). The experimentally measured stiffness, S, and the projected area of elastic contact, A (based on the indentation depth and determined from the tip area function), are used to determine the reduced modulus, E_r, according to the equation

$$E_r = S\frac{\sqrt{\pi}}{2\sqrt{A}} \tag{1}$$

The effect of the non-rigidity of the indenter on the load-displacement behavior is accounted for by the use of a reduced modulus, E_r, through the equation

$$\frac{1}{E_r} = \frac{(1-\nu^2)}{E} + \frac{(1-\nu_i^2)}{E_i} \tag{2}$$

where E and ν are Young's modulus and Poisson's ratio for the specimen and Ei and νi are the same parameters for the indenter. The properties of the diamond indenter are known (Ei = 1140 GPa and νi = 0.07) and can be used to calculate a value of indentation modulus, ENI, from a nanoindentation measurement and Eqn. 1 and 2:

$$E_{NI} = \frac{E}{1-\nu^2} \tag{3}$$

Since no data or estimates could be found in the literature for the Poisson's ratio of kerogen, all elastic moduli reported here are indentation moduli. These results can be used to calculate a Young's modulus for kerogen in Woodford shale if knowledge of the Poisson's ratio becomes available.

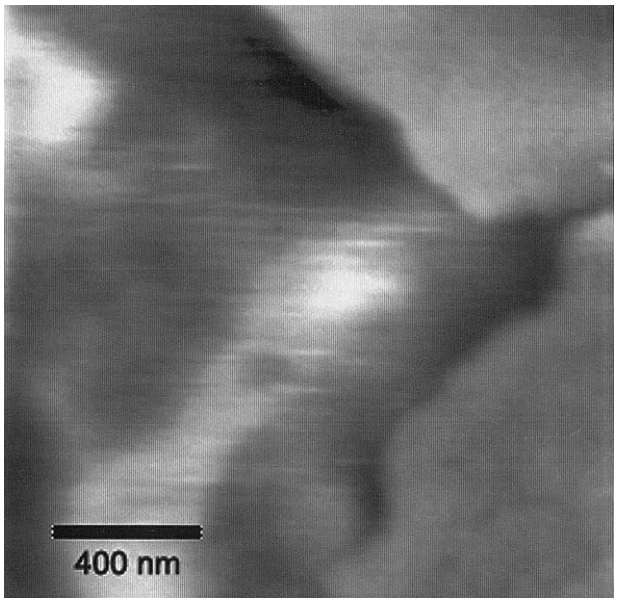

Fig. 2. An AFM image of kerogen within Woodford shale. Rippled region in center is indicative of kerogen. Smooth features in the top right and bottom right corners are typical of mineral phases.

The hardness, H, is defined as the mean pressure the material will support under load, and is computed from

$$H = \frac{P_{max}}{A} \tag{4}$$

where P_{max} is the maximum load.

3. RESULTS

An image of the rock surface generated by scanning the nanoindenter tip over the surface is shown in Figure 2. Contrast between the rock and the kerogen is due to the inherent difference in polishing traits between the softer macromolecular kerogen and the harder mineral phases. While the harder mineral phases polished well and achieved extremely smooth surfaces, the polished kerogen displayed a characteristically rippled surface. These ripples were randomly oriented and did not correspond to the scan direction and are thus unlikely to be the result of systematic errors associated with tip-surface interactions. Combining the observable contrast with the submicron resolution of atomic force microscopy, small regions of kerogen within the rock matrix were imaged and identified. After an indentation measurement, AFM imaging was also used to examine the residual indentation. Due to the low loads used, the residual impressions were either quite small or absent with only some additional surface roughness at the location of the indentation. An image of the residual impression left after nanoindentation into kerogen is shown in Figure 3. This observation indicates primarily elastic deformation for the loads used. Despite the absence of a large residual indentation, images of the kerogen and surrounding region before and after the test were found to be sufficient to verify the location of the indentation.

Hardness and indentation modulus results are given in Table 1 for orthogonal indentations of kerogen. Measurements were made on samples that correspond to three orthogonal faces of a

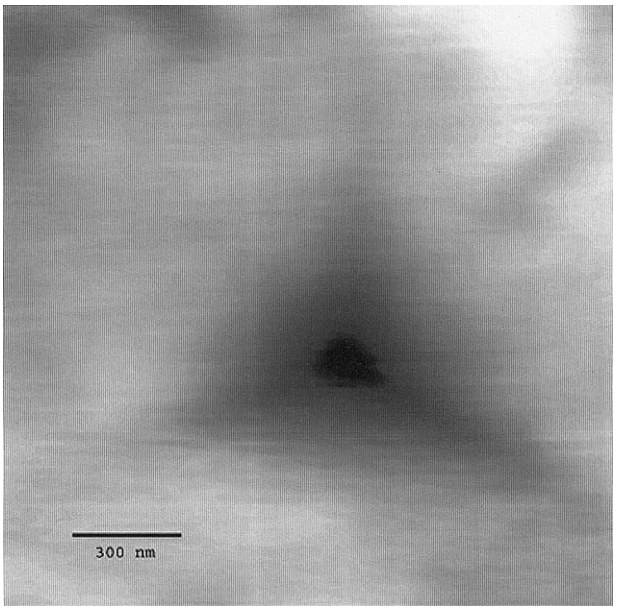

Fig. 3. An AFM image of kerogen after nanoindentation.

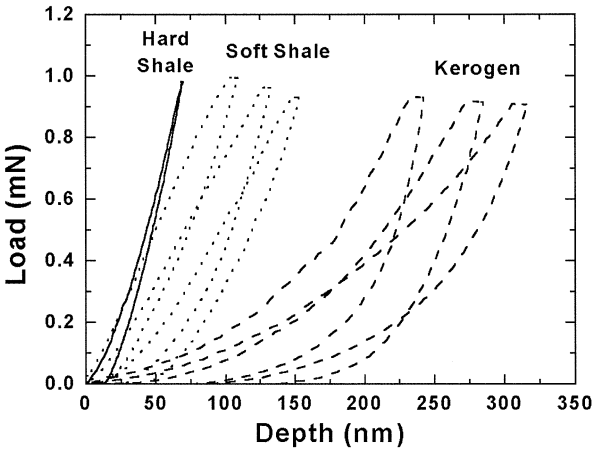

Fig. 4. Force versus displacement data for 7 indentations showing spread of data depending on the phase indented. The curve on the left is considered hard mineral phase, the 3 curves in the center soft mineral phase, and the 3 curves on the right are considered kerogen.

cube. Within a 95% confidence interval, no differences are found in the results for these three samples. Because the data is consistent regardless of the direction of the indentation relative to the bedding plane, the physical properties of this Woodford shale kerogen were found to be isotropic.

4. DISCUSSION

4.1. Validation of Nanoindentation Measurements

The experimental system proved capable of determining the physical properties of the kerogen without requiring extraction from the matrix. Plotting the load-displacement curves shows how the indentations fell into three groups (Fig. 4). Combining image information with the calculated hardness allowed us to confidently define the three groups as hard mineral phases (hardness $>$ 6 GPa and a smooth surface), softer mineral phases (hardness between 1 and 6 GPa and a smooth surface), or kerogen (hardness $<$ 1 GPa and a rippled surface). The distinct groupings shown in these curves is consistent with the heterogeneous nature of Woodford shale. One would expect properties for hard mineral phases, such as quartz, amorphous silica, and pyrite, would differ from softer mineral phases, like clays, and vary considerably from the even softer kerogen.

Table 1. Hardness and Indentation Modulus of Kerogen within Woodford Shale ($\pm$95% confidence limits).

	No. of Indents	Hardness (GPa)	Indentation Modulus (GPa/(1−ν^2))
Sample 1 Indentation Perpendicular to Bedding Plane	40	0.57 ± 0.03	10.5 ± 0.7
Sample 2 Indentation Parallel to Bedding Plane	29	0.55 ± 0.02	10.5 ± 1.0
Sample 3 Indentation Parallel to Bedding Plane	49	0.56 ± 0.03	11.1 ± 0.6

Measurements were made on samples that correspond to three orthogonal faces of a cube.

The measurement of indentation data for the kerogen regions dispersed within the shale required careful selection of indentation sites and validation of the load-displacement curves produced. Large area AFM scans were performed to find homogenous zones with the rippled surface indicative of kerogen. The tip was then centered over these regions and indentations performed. These efforts ensured that the test area was kerogen, at least at the surface, and that the neighboring matrix minimally affected the results. For example, indentation into a rippled kerogen area approximately 1 micron from its border with a hard mineral phase provided hardness and modulus values consistent with the overall results.

In indentations of a softer material that lies over a harder substrate, there is concern that the values determined for the softer material are affected by the substrate. To minimize this effect, a general rule is to keep indent depths at less than 10% of layer thickness to minimize substrate effects. In a natural sample such as Woodford shale, depths of kerogen domains are unknown and highly variable and it is impossible to follow the 10% rule. Therefore, there is no way to be sure what contribution, if any, substrate effects have on the data. Variability in the data (cf. Fig. 4) could be due to the natural variability of the kerogen in the sample or it could be due a varying influence of the substrate on the nanoindentation measurements. Thus, to minimize any potential for substrate effects, indentations were kept relatively shallow, at generally less than 400 nm.

A number of methods were used to elucidate any substrate effects on our indentation data. Since nanoindentation in a soft material on a hard substrate can induce pileup that greatly affects the calculated area and may render the results calculated by the Oliver and Pharr method erroneous, the residual imprint after indentation was visually examined and no evidence of

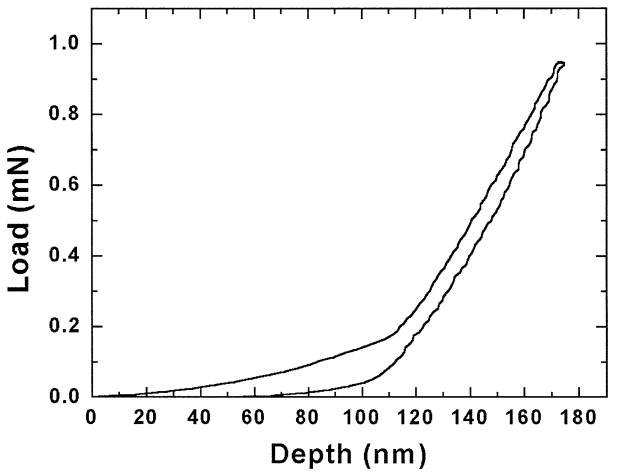

Fig. 5. Force versus displacement data for an indentation showing a distinct change in slope consistent with indentation of a hard material through a softer over-layer.

pileup was observed. As a further check for substrate effects, the load-displacement curves were examined for anomalous behavior. Indentation of a hard material through a thin softer over-layer will yield a load-displacement curve with a distinct slope discontinuity (Finke et al., 2001). Curves that exhibited this behavior in our case (Fig. 5) were presumed to be indentations made into an area where the kerogen was a thin layer over some mineral phase and these data were discarded. The load-displacement curves for kerogen in Figure 4 display no evidence of slope discontinuity and are indicative of those seen throughout the study. Finally, indentations made with lesser loads and shallower depths were also consistent with the reported results, further indicating a lack of substrate effects (cf. Table 1).

4.2. Anisotropy

Nanoindentation has been employed effectively for the study of anisotropic systems in materials science (Meng and Eesley, 1995; Turner et al., 1999). Data analysis procedures for hardness calculations do not need to change for anisotropic systems. Since data analysis procedures for determining elastic moduli strictly apply only to isotropic media (Oliver and Pharr, 1992), their use for anisotropic systems creates a slight bias toward underestimation of the anisotropy of Young's modulus (Hay et al., 1998). Thus, any anisotropy detected in the indentation modulus may be indicative of a slightly larger anisotropy in Young's modulus. Nanoindentation has detected hardness anisotropy as low as 20% and Young's modulus anisotropy as low as 6% in a study of nanolaminated films (Farhat et al., 1997).

Detection of anisotropy is of particular interest in this study. Since kerogen is an amorphous polymer, if the kerogen in Woodford shale were weight bearing, it would be expected that the pressure from the rock overburden would be acting upon the kerogen. This pressure, directional toward the center of the earth, should induce order in the macromolecular solid. This order should be exhibited as anisotropy in the physical properties and should be detectable by hardness and indentation modulus measurements. On the other hand, the rock may be load bearing and the kerogen subject to the isotropic pressure of pore fluids. Fluid pressure by its nature is the same in all directions and would lead to isotropic physical properties. The data contained in Table 1 show that within a 95% confidence limit, the indentation modulus and hardness of Woodford kerogen is the same parallel and perpendicular to the bedding plane. This result indicates that there is no detectable anisotropy in kerogen mechanical properties and there is no evidence for overburden pressure on this immature kerogen.

The conclusion that there is no evidence that this kerogen in Woodford shale has experienced overburden pressure also assumes that mechanical anisotropy induced by this pressure would be preserved in the kerogen during sample preparation and storage. If the sample was warmed for long enough under isotropic pressure conditions, its structure could relax and the anisotropy could be lost. This restructuring would happen quickly if the kerogen was heated above its T_g, so samples were stored at ambient temperature and no thermal studies were performed on these samples. Another possibility for loss of anisotropy is surface annealing during cutting and polishing. These processes generate heat, perhaps enough to allow the kerogen to relax. These processes are not expected to provide sufficient thermal energy to anneal the kerogen of anisotropic properties, since more extensive handling (ultrasonic dispersion and ball-mill homogenization) showed no disturbance of the chemical structure of organic matter in a geochemical sample reported in the literature (Schmidt et al., 1997). Relaxation might also occur if the sample is at a temperature below its T_g but warm enough to allow reorganization on a slow but significant time scale. We plan to test the effect of temperature on the determination of mechanical properties in our next series of measurements.

4.3. Mechanical Properties

The mechanical properties of this kerogen are unique for a polymer. Woodford shale kerogen is hard (550 MPa hardness), much harder than common hard polymers (polymethylmethacrylate, polycarbonate, phenolics) that typically have hardness of below 200 MPa. The hardness of this kerogen is closer to that of a soft mineral such as gypsum or a soft metal such as tin or gold. This kerogen also exhibits both elasticity and plasticity. It is somewhat elastic, having recovered a significant part of the deformation, but it also was irreversibly deformed. Although it was not rigorously studied, the samples displayed evidence of viscoelastic recovery, as there was a time dependent loss of some of the residual imprint. It will be interesting to see if kerogen from other sources show similar behavior and whether mature kerogen shows signs of overburden pressure.

5. CONCLUSIONS

This study shows the application of combined nanoindentation and AFM imaging to the analysis of a mechanically heterogeneous geological sample. Kerogen was successfully imaged within the matrix of Woodford shale with contrast due to inherent polishing differences of the phases. This allowed the analysis of specific kerogen domains. Nanoindentation measurements showed kerogen within Woodford shale to be a very

hard material (relative to other polymers) that behaves both elastically and plastically. The results show no evidence of anisotropy in the physical properties of kerogen within Woodford shale at this level of thermal maturity. Future studies will examine whether there is evidence of anisotropy at higher levels of thermal maturity.

Acknowledgments—Acknowledgment is made to the Donors of the Petroleum Research Foundation, administered by the American Chemical Society, for partial support of this research. Support by the National Science Foundation is also gratefully acknowledged. The authors gratefully acknowledge donated instrument time and helpful discussions with individuals at Hysitron, Inc., including Thomas Wyrobek, Dehau Yang, Lance Kuhn and Tony Anderson.

Associate editor: R. C. Burruss

REFERENCES

Andrews R. D. (1954) Measurement of Orientation in Polystyrene Monofilaments by Means of Double Refraction. *J. Appl. Phys.* **25,** 1223–1231.

Bhushan B., Kulkarni A. V., Bonin W., and Wyrobek J. T. (1996) Nanoindentation and picoindentation measurements using a capacitive transducer system in atomic force microscopy. *Phil. Mag. A.* **74,** 1117–1128.

Blanc P. and Connan J. (1992) Generation and Expulsion of Hydrocarbons from a Paris Basin Toarcian Source Rock: An Experimental Study by Confined-System Pyrolysis. *Energy and Fuels* **6,** 666–677.

Burnham A. K. and Braun R. L. (1990) Development of a detailed model of petroleum formation, destruction, and expulsion from lacustrine and marine source rocks. *Org. Geochem.* **16,** 27–39.

Burruss R. C. and Hatch J. R. (1989) Geochemistry of oils and hydrocarbon source rocks, greater Anadarko basin: evidence for multiple sources of oils and long-distance oil migration. *Oklahoma Geol. Surv. Circ.* **90,** 53–64.

Cardott B. J. and Lambert M. W. (1985) Thermal maturation by vitrinite reflectance of Woodford shale, Anadarko Basin, Oklahoma. *Am. Ass. Petr. Geol. Bull.* **69,** 1982–1998.

Cardott B. J. (1989) Thermal maturation of the Woodford Shale in the Anadarko Basin. *Oklahoma Geol. Surv. Circ.* **90,** 32–46.

Cardott B. J., Metcalf W. J., III, and Ahern J. L. (1990) Thermal maturation by vitrinite reflectance of Woodford Shale near Washita Valley fault, Arbuckle Mountains, Oklahoma. In *Applications of thermal maturity studies to energy exploration* (eds. V. F. Nuccio, C. E. Barker, and S. J. Dyson), pp. 139–146. Eastwood Print. and Publ, Denver CO.

Chen X. and Vlassak J. (2001) A finite element study on the nanoindentation of thin films. In *Fundamentals of Nanoindentation and Nanotribology II, Mater. Res. Soc. Proc.* vol. 649 (eds. S. P. Baker, R. F. Cook, S. G. Corcoran, and N. R. Moody). pp. Q.1.3.1-Q.1.3.6. Materials Research Society, Pittsburgh, PA.

Cody G. D., Jr., Larsen J. W., and Siskin M. (1988) Anisotropic Solvent Swelling of Coals. *Energy and Fuels* **2,** 340–344.

Comer J. B. and Hinch H. H. (1987) Recognizing and quantifying expulsion of oil from the Woodford formation and age-equivalent rocks in Oklahoma and Arkansas. *Am. Ass. Petr. Geol. Bull.* **71,** 844–858.

Donath E. (2001) The Glass Transition. Springer, New York.

Farhat Z. N., Ding Y., Northwood D. O., and Alpas A. T. (1997) Nanoindentation and friction studies on Ti-based nanolaminated films. *Surf. Coat. Technol.* **89,** 24–30.

Fett T., Nothdurft W., and Racke H. H. (1973) Determination of Knoop hardness for determining the states of orientation of amorphous thermoplastics. *Kunststoffe* **63,** 107–110.

Finke M., Hughes J. A., Parker D. M., and Jandt K. D. (2001) Mechanical properties of in situ demineralised human enamel measured by AFM nanoindentation. *Surf. Sci.* **491,** 456–467.

Fischer-Cripps A. C. (2002) Nanoindentation. Springer-Verlag, New York.

Göklen K. E., Stoecker T. J., and Baddour R. F. (1984) A Method for the Isolation of Kerogen from Green River Oil Shale. *Ind. Eng. Chem. Prod. Res. Dev.* **23,** 308–311.

Hanebeck D. (1995) Experimental simulation and study of the genesis and expulsion of petroleums from source rocks. Berichte des Forschungszentrums Juelich. *JUEL* **3048,** 326.

Hay J. C., Sun E. Y., Pharr G. M., Becher P. F., and Alexander K. B. (1998) Elastic Anisotropy of β-Silicon Nitride Whiskers. *J. Am. Cer. Soc.* **81,** 2661–2669.

JohnsonK. S. and CardottB. J. (1992) Geologic framework and hydrocarbon source rocks of Oklahoma. In *Source Rocks in the Midcontinent, 1990 Symposium* (eds. K. S. Johnson and B. J. Cardott) *Oklahoma Geol. Surv. Circ.* **93,** 21–37.

Jones P. J. (1986) The petroleum geochemistry of the Pauls Valley area, Anadarko basin, Oklahoma. Dissertation, Oklahoma University.

Jones P. J. and Philp R. P. (1990) Oils and source rocks from the Pauls Valley, Anadarko Basin, Oklahoma, USA. *Appl. Geochem.* **5,** 429–448.

Kempe A., Schopf J. W., Altermann W., Kudryavtsev A. B., and Heckl W. M. (2002) Atomic force microscopy of Precambrian microscopic fossils. *Proc. Natl. Acad. Sci.* **99,** 9117–9120.

Khorasani G. K, Michelsen J. K (1995) Overpressure: Effect on petroleum generation. *Organic Geochemistry: Developments and Applications to Energy, Climate, Environment and Human History,* 17th International Meeting on Organic Geochemistry (eds. Grimalt J. O. and Dorronsoro) A I.G.O.A., Spain, 560–562.

Kirkland D. W., DenisonR.E., Summers D. M., Gormly J. R. (1992) Geology and organic geochemistry of the Woodford shale in the Criner Hills and Western Arbuckle Mountains. In *Source Rocks in the Midcontinent, 1990 Symposium* (eds. K. S. Johnson and B. J. Cardott) *Oklahoma Geol. Surv. Circ.* **93,** 38–69.

Lewan M. D., Winters J. C., and McDonald J. H. (1979) Generation of Oil-Like Pyrolyzates from Organic-Rich Shales. *Science* **203,** 897–899.

Meng W. J. and Eesley G. L. (1995) Growth and mechanical anisotropy of TiN thin films. *Thin Solid Films* **27,** 108–116.

Michels R., Landais P., Philp R. P., and Torkelson B. (1994) Effects of pressure on organic matter maturation during confined pyrolysis of Woodford kerogen. *Energy and Fuels* **8,** 741–754.

Michels R., Landais P., Torkelson B. E., and Philp R. P. (1995a) Effects of confinement and water pressure on oil generation during confined pyrolysis, hydrous pyrolysis and high pressure hydrous pyrolysis. *Geochim. Cosmochim. Acta* **59,** 1589–1604.

Michels R., Landais P., Philp R. P., and Torkelson B. E. (1995b) Influence of Pressure and the Presence of Water on the Evolution of the Residual Kerogen during Confined, Hydrous, and High-Pressure Hydrous Pyrolysis of Woodford Shale. *Energy and Fuels* **9,** 204–215.

Morgans W. T. A. and Terry N. B. (1958) Measurements of the Static and Dynamic Elastic Moduli of Coal. *Fuel* **37,** 201–219.

Oliver W. C. and Pharr G. M. (1992) An improved technique for determining hardness and elastic modulus using load and displacement sensing indentation experiments. *J. Mater Res.* **7,** 1564–1583.

Parks T. J., Lynch L. J., Webster D. S., and Barrett D. (1988) Molecular Properties and Thermal Transformations of Oil Shale Kerogens from in situ 1H NMR Data. *Energy and Fuels* **2,** 185–190.

Philp R. P., Chen J., Galvez-Sinibaldi A., Wang H., Allen J. D. (1992) Effects of weathering and maturity on the geochemical characteristics of the Woodford shale. In *Source Rocks in the Midcontinent, 1990 Symposium* (eds. K. S. Johnson and B. J. Cardott) *Oklahoma Geol. Surv. Circ.* **93,** 38–69.

Philp R. P., Jones P. J., Lin L. H., Michael G. E., and Lewis C. A. (1989) An organic geochemical study of oils, source rocks and tar sands in the Ardmore and Anadarko basins. *Oklahoma Geol. Surv. Circ.* **90,** 65–76.

Reber J. (1989) Biomarker characterization of Woodford-type oil and correlation to source rock, Aylesworth field, Marshall county, Oklahoma. *Oklahoma Geol. Surv. Circ.* **90,** 271.

Rice D. D., Threlkeld C. N., and Vuletich A. K. (1989) Characterization and origin of natural gases of the Anadarko basin. *Oklahoma Geol. Surv. Circ.* **90,** 47–52.

Rudkiewicz J. L., Brevart O., Connan J., and Montel F. (1994) Primary migration behavior of hydrocarbons: from laboratory experiments to geological situations through fluid flow models. *Org. Geochem.* **22,** 631–639.

Saxby J. D. (1970) Isolation of kerogen in sediments by chemical methods. *Chem. Geol.* **6,** 173–184.

Schmidt M. W. I., Knicker H., Hatcher P. G., and Kögel-Knabner I. (1997) Does ultrasonic dispersion and homogenization by ball milling change the chemical structure of organic matter in geochemical samples?—a CPMAS., 13C NMR study with lignin. *Org. Geochem.* **26,** 491–496.

Schmoker J. W. and Hester T. C. (1989) Formation resistivity as an indicator of the onset of oil generation in the Woodford Shale, Anadarko Basin, Oklahoma. *Oklahoma Geol. Surv. Circ.* **90,** 262–266.

Smith T. (1989) Evidence of early oil generation in the Woodford Shale, Witcher Field, Central Oklahoma. *Oklahoma Geol. Surv. Circ.* **90,** 267.

Tsui T. Y., Vlassak J., and Nix W. D. (1999) Indentation plastic displacement field: Part I. The case of soft films on hard substrates. *J. Mater. Res.* **14,** 2196–2203.

Turner C. H., Rho J., Takano Y., Tsui T. Y., and Pharr G. M. (1999) The elastic properties of trabecular and cortical bone tissues are similar: results from two microscopic measurement techniques. *J Biomech.* **32,** 437–441.

van Krevelen D. W. (1960) Coal. Elsevier. Amsterdam.

Villey M., Oberlin A., and Combaz A. (1979) Influence of Elemental Composition on Carbonization Pyrolysis of Spporopollenin and Lignite as Models of Kerogens. *Carbon.* **17,** 77–86.

Vlassak J. J. and Nix W. D. (1993) Indentation modulus of elastically anisotropic half spaces. *Phil. Mag. A.* **67,** 1045–1056.

Vlassak J. J. and Nix W. D. (1994) Measuring the elastic properties of anisotropic materials by means of indentation experiments. *J. Mech. Phys. Solids* **42,** 1223–1245.

Wang L. (1989) Modeling of hydrocarbon generation and migration for the Woodford Shale in the Anadarko Basin. *Oklahoma Geol. Surv. Circ.* **90,** 268–270.

Yamada O., Zabat M., Yasuda H., Zhang A., Nakano K., and Kaiho M. (2000) Use of atomic force microscope for the study of mechanical properties of coal surfaces. *Sekitan Kagaku Kaigi Happyo Ronbunshu.* **37,** 11–14.